Inclusion properties of palladium(II) and platinum(II) hydroquinonylphosphine complexes: the molecular and crystal structures of *trans*-[PdCl₂(pphqH₂)₂] · (acetone)₂, *trans*-[PtCl₂(pphqH₂)₂] · (dimethylformamide)₄ and *trans*-[PdCl₂(pphqMe₂)₂]

Seri Bima Sembiring, Stephen B. Colbran *, Roger Bishop *, Donald C. Craig,
A. David Rae

School of Chemistry, University of New South Wales, Sydney, NSW 2052, Australia

Abstract

The X-ray single crystal structures of two *p*-hydroquinonylphosphine complexes, *trans*-[PdCl₂(pphqH₂)₂] (**1**) and *trans*-[PtCl₂(pphqH₂)₂] (**2**), and one *p*-hydroquinonyldimethyletherphosphine complex, *trans*-[PdCl₂(pphqMe₂)₂] (**3**), are described. **1** co-crystallizes with two molecules of lattice-included acetone ((**1**)·(acetone)₂) in the monoclinic space group $C2/m$ with $Z=2$ and cell constants $a = 13.857(6)$, $b = 13.589(3)$, $c = 11.863(5)$ Å, $\beta = 104.68(2)°$. Intermolecular hydrogen bonding between molecules of **1** leads to channels that run parallel to the c axis and which include the acetone guest molecules. Complex **2** co-crystallizes with four molecules of dimethylformamide solvent ((**2**)·(DMF)₄) in the triclinic space group $P\bar{1}$ with $Z=1$ and cell constants $a = 10.500(6)$, $b = 11.927(8)$, $c = 12.225(6)$ Å, $\alpha = 64.65(5)$, $\beta = 66.74(5)$, $\gamma = 78.84(5)°$. Each dimethylformamide molecule in (**2**)·(DMF)₄ is hydrogen bonded to one of the four O–H groups of **2**. Complex **3** crystallizes in the triclinic space group $P\bar{1}$ with $Z=1$ and cell constants $a = 9.063(5)$, $b = 10.548(7)$, $c = 11.596(8)$ Å, $\alpha = 111.57(3)$, $\beta = 111.26(3)$, $\gamma = 90.09(4)°$. It is shown that there is a close relationship between the molecular structures and the co-crystalline behavior of **1** and **2** and the molecular structures and inclusion properties of organic 'wheel-and-axle' host molecules. The analogy is extended to provide some guidelines for the design of new inorganic host molecules.

Keywords: Crystal structures; Palladium complexes; Platinum complexes; Hydroquinonylphosphine complexes

1. Introduction

We have recently reported the stepwise syntheses of platinum and palladium complexes with electrochemically active *p*-benzoquinonylphosphine ligands from *p*-hydroquinonylphosphine and *p*-dimethoxyphenylphosphine precursor complexes [1,2]. Phenolic compounds often crystallize with open structures which optimize dipolar hydrogen bonding interactions but do not give efficient molecular packing and thus leave quite large cavities or holes or channels in the open three-dimensional molecular lattice in which other molecules can be trapped [3]. For example, lattice inclusion compounds (clathrates) of *p*-hydroquinone [1,4-C₆H₄(OH)₄] have been prepared enclosing gases (e.g. SO₂, H₂S, HCl, CO, Ar, Kr,) and solvents (e.g. MeOH, MeCN) [4]. In recent elegant work, Ermer has demonstrated that larger molecules, C₆₀ in fact, may be included in a single cubic superpolonium parahydroquinonyl net [5]. On the other hand, substituted hydroquinones do not usually include guest molecules [3–6]. It was therefore interesting to find that the hydroquinonylphosphine platinum and palladium complexes crystallized with incorporated (hydrogen bonded) solvent. Herein, the X-ray crystal and molecular structures of the *p*-hydroquinonylphosphine complexes *trans*-[PdCl₂(pphqH₂)₂] · (acetone)₂ ((**1**) · (acetone)₂) and *trans*-[PtCl₂(pphqH₂)₂] ·

Abbreviations: diphenylphosphino-*p*-hydroquinonyldimethylether (pphqMe₂); diphenylphosphino-*p*-hydroquinone (pphqH₂); dimethylformamide (DMF).

* Corresponding authors.

(dimethylformamide)$_4$ ((2)·(DMF)$_4$) are reported along with the X-ray crystal and molecular structure of the p-dimethoxyphenylphosphine complex, trans-[PdCl$_2$(pphqMe$_2$)$_2$] (3), for comparison. It is shown that (1)·(acetone)$_2$ is a lattice inclusion compound whereas (2)·(DMF)$_4$ is not. A priori design of inorganic host molecules presents a considerable challenge [6]. However, it is suggested the present co-crystalline behavior of 1 and 2 occurs because the molecules have structures that are closely related to organic 'wheel-and-axle' host molecules [7–10]. Extension of this analogy leads to some guidelines for the design of potential new inorganic host compounds.

2. Results

2.1. X-ray crystallography

Yellow crystals of (1)·(acetone)$_2$ were obtained by slow evaporation of an acetone solution. Pale yellow (2)·(DMF)$_4$ crystallized on cooling a dimethylformamide solution and orange crystals of 3 were grown from a concentrated dichloromethane solution. Atom coordinates, and bond length and bond angle data from the single crystal X-ray structure determinations for 1–3 are presented in Tables 1–9.

2.1.1. Molecular structures

All three complexes, 1–3, have a crystallographic inversion center sited at the metal atom. It is immediately apparent that all three complexes have trans-coordinated ligands (Figs. 1–3). Each complex has a skewed square planar geometry about the metal atom. Although both chloro and both phosphine ligands are exactly trans to
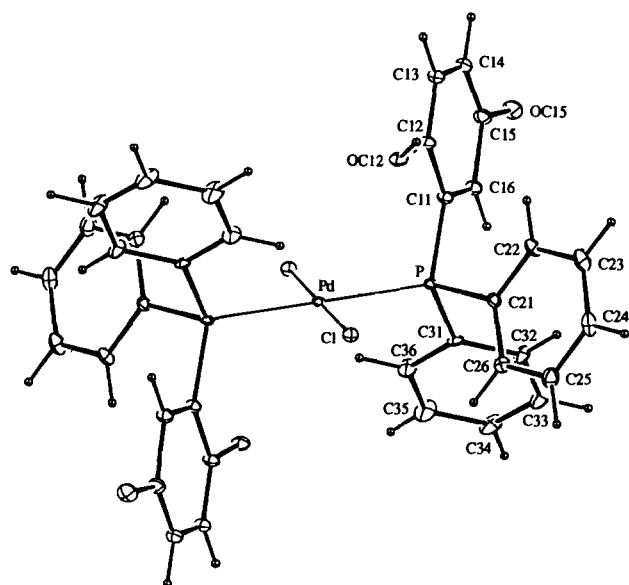

Fig. 1. ORTEP diagram (10% thermal elipsoids) showing the molecular structure of 1.

Table 1
Non-hydrogen atomic parameters for (1)·(acetone)$_2$ with e.s.d.s in parentheses

	x	y	z	U_{iso} [a]
Pd	0.5000	0.00000	0.500	0.026(1)
Cl	0.6676(2)	−0.0227(2)	0.5830(3)	0.038(1)
P	0.4620(2)	−0.0164(4)	0.6806(2)	0.026(1)
OC12	0.4801(6)	−0.2208(6)	0.6117(6)	0.043(2)
OC15	0.1286(7)	−0.1493(8)	0.7421(7)	0.060(3)
C11	0.3702(5)	−0.1144(6)	0.6788(4)	0.034(2)
C12	0.3887(8)	−0.2075(10)	0.6440(6)	0.038(2)
C13	0.3237(11)	−0.2830(11)	0.6403(7)	0.044(2)
C14	0.2378(10)	−0.2642(11)	0.6725(7)	0.047(2)
C15	0.2164(8)	−0.1754(11)	0.7070(6)	0.046(2)
C16	0.2841(9)	−0.0931(9)	0.7120(6)	0.039(2)
C21	0.5672(5)	−0.0403(4)	0.8074(6)	0.034(2)
C22	0.5717(7)	−0.1277(7)	0.8671(8)	0.048(2)
C23	0.6522(9)	−0.1457(9)	0.9648(10)	0.062(3)
C24	0.7236(6)	−0.0745(7)	0.9970(7)	0.059(3)
C25	0.7198(6)	0.0131(10)	0.9380(8)	0.058(3)
C26	0.6400(6)	0.0301(7)	0.8415(7)	0.046(2)
C31	0.4060(4)	0.0965(6)	0.7211(4)	0.031(3)
C32	0.4095(7)	0.1142(7)	0.8362(8)	0.049(3)
C33	0.3668(9)	0.2010(9)	0.8676(11)	0.068(4)
C34	0.3229(7)	0.2652(6)	0.7810(9)	0.070(4)
C35	0.3189(10)	0.2484(7)	0.6656(13)	0.078(5)
C36	0.3614(8)	0.1624(7)	0.6356(9)	0.055(4)

[a] $U_{iso} = 1/3(U_{11} + U_{22} + U_{33})$.

Table 2
Bond lengths (Å) for (1)·(acetone)$_2$ with e.s.d.s in parentheses

Cl–Pd	2.302(3)	P–Pd	2.343(3)
C11–P	1.838(8)	C12–OC12	1.424(12)
C12–C11	1.374(16)	C13–C12	1.359(19)
C14–C13	1.363(22)	C15–OC15	1.428(12)
C15–C14	1.332(20)	C16–C11	1.378(14)
C16–C15	1.452(18)	C21–P	1.838(7)
C22–C21	1.376(8)	C23–C22	1.411(13)
C24–C23	1.367(11)	C25–C24	1.375(9)
C26–C21	1.376(8)	C26–C25	1.394(10)
C31–P	1.837(7)	C32–C31	1.376(8)
C33–C32	1.411(13)	C34–C33	1.367(11)
C35–C34	1.375(9)	C36–C31	1.376(8)
C36–C35	1.394(10)		

each other in each complex, the skewed geometry about the metal atom results in two P–M–Cl angles of 88.1(1) and 91.9(1)° for 1, 87.2(1) and 92.8(1)° for 2, and 85.9(1) and 94.1(1)° for 3. The Pd–Cl and Pd–P bond distances, 2.302(3) and 2.343(3) Å for 1 and 2.307(1) and 2.337(1) Å for 3, and the Pt–Cl and Pt–P bond distances of 2.379(1) and 2.319(2) Å for 2, are all unremarkable and comparable to analogous distances in other palladium(II) and platinum(II) phosphine complexes [11]. In 1 the p-hydroquinonyl substituents adopt the conformation that minimizes the non-bonding distance between the palladium and the ortho-OH groups, i.e. structure I as opposed to structure II in Fig. 4. In 3 the same conformation is adapted by the hydroqui-
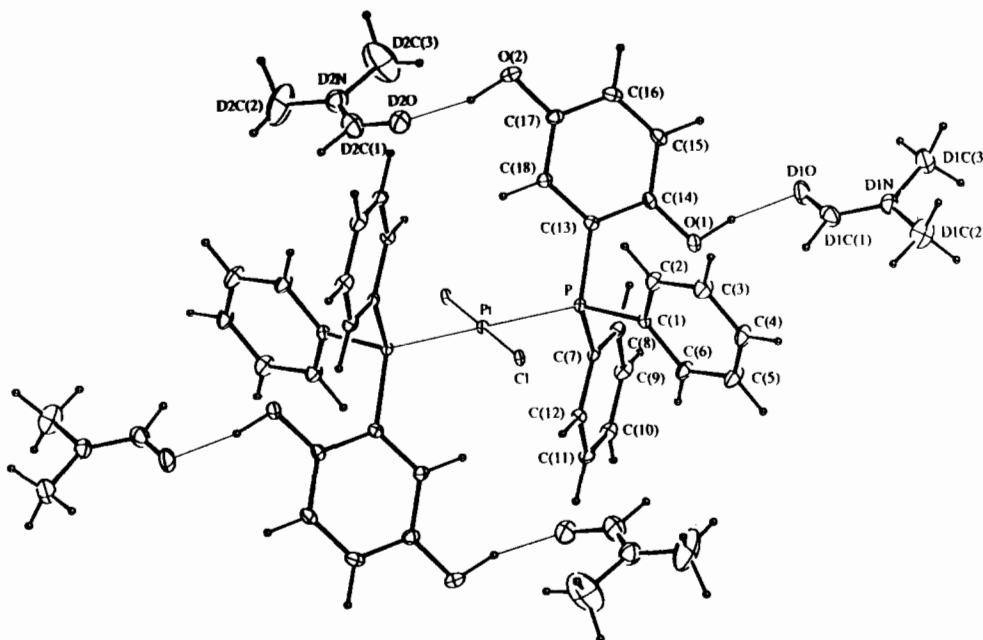
Fig. 2. ORTEP diagram (10% thermal elipsoids) showing the molecular structure of 2 and the four hydrogen bonded dimethylformamide molecules.
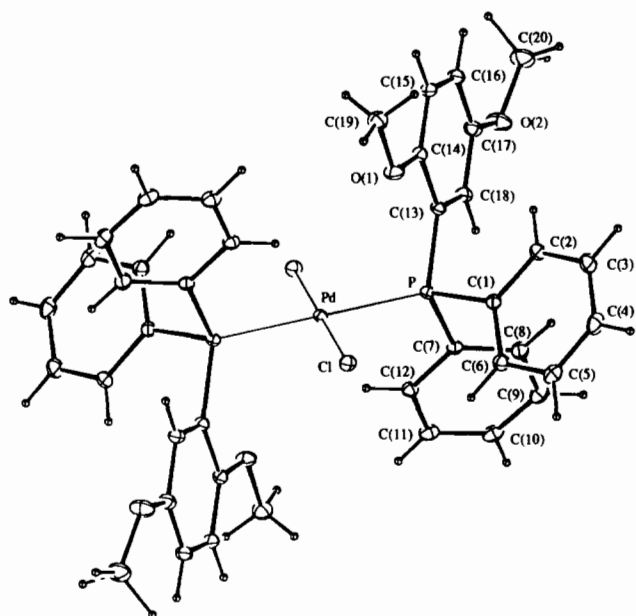

Fig. 3. ORTEP diagram (10% thermal elipsoids) showing the molecular structure of 3.

Table 3
Bond angles (°) for (1)·(acetone)$_2$ with e.s.d.s in parentheses

Cl–Pd–P	91.9(1)	Cl–Pd–P [a]	88.1(1)
OC12–Cl–OC12 [a]	110.6(2)	Pd–P–C11	112.0(2)
Pd–P–C21	116.7(2)	Pd–P–C31	111.5(2)
C11–P–C21	106.5(2)	C11–P–C31	105.8(2)
C21–P–C31	103.5(2)	Cl–OC12–C12	127.3(7)
P–C11–C12	119.3(5)	P–C11–C16	119.4(5)
C12–C11–C16	121.4(10)	OC12–C12–C11	116.3(10)
OC12–C12–C13	121.5(12)	C11–C12–C13	122.1(11)
C12–C13–C14	117.9(14)	C13–C14–C15	122.3(13)
OC15–C15–C14	126.0(13)	OC15–C15–C16	112.8(12)
C14–C15–C16	121.2(12)	C11–C16–C15	115.1(10)
P–C21–C22	119.8(4)	P–C21–C26	119.2(4)
C22–C21–C26	121.0(8)	C21–C22–C23	119.7(8)
C22–C23–C24	118.2(9)	C23–C24–C25	122.6(6)
C24–C25–C26	118.8(7)	C21–C26–C25	119.7(8)
P–C31–C32	119.6(5)	P–C31–C36	119.4(4)
C32–C31–C36	121.0(8)	C31–C32–C33	119.7(8)
C32–C33–C34	118.2(9)	C33–C34–C35	122.6(6)
C34–C35–C36	118.8(7)	C31–C36–C35	119.7(8)
C15–OC15–OC12 [b]	103.8(7)	OC15–OC12 [b]–C12	120.1(5)

Superscripts indicate the symmetry transformations: [a] $1-x$, $-y$, $1-z$; [b] $-\frac{1}{2}+x$, $-\frac{1}{2}-y$, z.

nonyldimethyl ether substituents. The distance between the *ortho*-oxygen and metal atom is 3.319 Å in 1 and 3.368 Å in 3. We suggest that this long, formally non-bonding interaction between the electron-rich *ortho*-oxygen and electropositive metal atoms is weakly attractive in nature, and in the absence of more favorable interactions to the oxygen atoms (vide infra), stabilizes structure I over structure II. Other investigators of *ortho*-methoxyphenyl- or *ortho*-hydroxyphenylphosphine complexes have also found long, formally non-bonding interactions between *ortho*-oxygen and metal atoms that

appear weakly attractive in nature [12]. Two molecules of acetone, that were not successfully modelled, occur in the region that extends beyond the *meta*-OH groups of 1 and likely are involved in hydrogen bonding with these OH groups (see below). The hydroquinonyl substituents in 2 are both orientated such that the *ortho*-OH group points away from the platinum atom (i.e. structure II in Fig. 4). All four hydroquinonyl OH groups in 2 are hydrogen bonded to a molecule of dimethylformamide (Fig. 2). The metal atom and phos-

Table 4
Non-hydrogen atomic parameters for $(2)\cdot(DMF)_4$ with e.s.d.s in parentheses

	x	y	z	B_{eq} [a]
Pt	0.5000	0.5000	0.5000	2.59(1)
Cl	0.7234(1)	0.5530(1)	0.3379(1)	2.42(5)
P	0.3889(2)	0.5913(2)	0.3504(2)	2.64(6)
O(1)	0.2184(7)	0.7590(5)	0.1891(6)	4.88(24)
O(2)	0.2054(8)	0.9172(6)	0.5563(7)	6.38(31)
C(1)	0.4984(7)	0.6591(6)	0.1787(6)	3.09(24)
C(2)	0.5621(10)	0.7689(8)	0.1329(8)	4.76(33)
C(3)	0.6363(11)	0.8268(9)	0.0047(9)	5.86(40)
C(4)	0.6545(11)	0.7761(10)	−0.0803(8)	5.72(39)
C(5)	0.5929(13)	0.6657(11)	−0.0361(9)	6.70(46)
C(6)	0.5186(11)	0.6069(9)	0.0921(8)	5.18(35)
C(7)	0.2892(7)	0.4736(6)	0.3643(6)	3.00(23)
C(8)	0.1510(8)	0.4920(7)	0.3725(7)	3.79(23)
C(9)	0.0808(9)	0.3960(9)	0.3890(9)	4.84(36)
C(10)	0.1461(10)	0.2826(9)	0.3947(8)	4.93(36)
C(11)	0.2829(11)	0.2651(7)	0.3837(8)	4.76(35)
C(12)	0.3565(9)	0.3603(7)	0.3691(7)	3.91(29)
C(13)	0.2794(7)	0.7245(6)	0.3693(7)	3.14(24)
C(14)	0.2138(8)	0.7991(7)	0.2786(7)	3.56(26)
C(15)	0.1480(8)	0.9099(7)	0.2853(8)	4.31(29)
C(16)	0.1452(9)	0.9484(7)	0.3778(9)	4.76(32)
C(17)	0.2104(8)	0.8752(7)	0.4667(8)	4.13(29)
C(18)	0.2747(7)	0.7641(7)	0.4627(7)	3.31(25)
D1O	0.1797(9)	0.9420(8)	−0.0117(7)	7.12(33)
D1N	0.2965(9)	1.0389(8)	−0.2288(8)	5.46(33)
D1C(1)	0.2831(14)	0.9576(11)	−0.1070(14)	6.95(59)
D1C(2)	0.4164(15)	1.0536(17)	−0.3409(14)	9.70(77)
D1C(3)	0.1799(14)	1.1145(13)	−0.2549(12)	8.03(58)
D2O	0.2956(11)	0.7538(10)	0.7424(10)	8.77(47)
D2N	0.1221(12)	0.6758(12)	0.9387(11)	8.07(53)
D2C(1)	0.2494(20)	0.6861(17)	0.8576(20)	10.16(94)
D2C(2)	0.0789(29)	0.5998(30)	1.0698(17)	18.47(99)
D2C(3)	0.0254(23)	0.7569(29)	0.8874(32)	20.81(99)

[a] B_{eq} (Å^2) is the isotropic equivalent of the anisotropic temperature factor.

Table 5
Bond lengths (Å) for $(2)\cdot(DMF)_4$ with e.s.d.s in parentheses

Pt–Cl	2.379(1)	C(14)–C(15)	1.387(11)
Pt–P	2.319(2)	C(15)–C(16)	1.380(13)
P–C(1)	1.839(7)	C(16)–C(17)	1.398(13)
P–C(7)	1.822(7)	C(17)–C(18)	1.378(11)
P–C(13)	1.815(7)	C(18)–C(13)	1.393(10)
C(1)–C(2)	1.375(11)	C(14)–O(1)	1.353(9)
C(2)–C(3)	1.363(12)	C(17)–O(2)	1.363(10)
C(3)–C(4)	1.348(13)	D1N–D1C(1)	1.352(15)
C(4)–C(5)	1.374(14)	D1N–D1C(2)	1.417(16)
C(5)–C(6)	1.364(12)	D1N–D1C(3)	1.431(15)
C(6)–C(1)	1.375(11)	D1C(1)–D1O	1.210(15)
C(7)–C(8)	1.395(10)	D2N–D2C(1)	1.302(22)
C(8)–C(9)	1.380(11)	D2N–D2C(2)	1.391(21)
C(9)–C(10)	1.380(13)	D2N–D2C(3)	1.401(24)
C(10)–C(11)	1.371(13)	D2C(1)–D2O	1.229(20)
C(11)–C(12)	1.407(11)	O(1)–D1O	2.609(9)
C(12)–C(7)	1.397(10)	O(2)–D2O	2.663(12)
C(13)–C(14)	1.419(10)		

Table 6
Bond angles (°) for $(2)\cdot(DMF)_4$ with e.s.d.s in parentheses

Cl–Pt–P	92.8(1)	C(7)–C(8)–C(9)	119.7(8)
Pt–P–C(1)	117.4(2)	C(8)–C(9)–C(10)	121.0(8)
Pt–P–C(7)	108.4(2)	C(9)–C(10)–C(11)	119.4(7)
Pt–P–C(13)	112.9(2)	C(10)–C(11)–C(12)	120.9(8)
C(1)–P–C(7)	105.7(3)	C(11)–C(12)–C(7)	119.0(8)
C(1)–P–C(13)	101.0(3)	P–C(13)–C(14)	120.7(5)
C(7)–P–C(13)	111.1(3)	C(18)–C(13)–P	119.7(5)
P–C(1)–C(2)	118.8(5)	C(18)–C(13)–C(14)	119.0(6)
C(6)–C(1)–P	123.5(6)	C(13)–C(14)–C(15)	118.9(7)
C(6)–C(1)–C(2)	117.7(7)	C(13)–C(14)–O(1)	118.4(6)
C(1)–C(2)–C(3)	120.8(8)	C(15)–C(14)–O(1)	122.7(7)
C(2)–C(3)–C(4)	121.3(8)	C(14)–C(15)–C(16)	121.4(7)
C(3)–C(4)–C(5)	118.7(8)	C(15)–C(16)–C(17)	119.7(7)
C(4)–C(5)–C(6)	120.4(8)	C(16)–C(17)–C(18)	119.7(7)
C(5)–C(6)–C(1)	120.9(8)	C(16)–C(17)–O(2)	117.5(7)
P–C(7)–C(8)	123.3(5)	C(18)–C(17)–O(2)	122.7(8)
C(12)–C(7)–P	116.8(6)	C(17)–C(18)–C(13)	121.2(7)
C(12)–C(7)–C(8)	119.9(7)		

Table 7
Non-hydrogen atomic parameters for 3 with e.s.d.s in parentheses

	x	y	z	B_{eq} [a]
Pd	0.5000	0.5000	0.5000	2.64(1)
Cl	0.3035(1)	0.6087(1)	0.3998(1)	3.72(2)
P	0.4622(1)	0.3161(1)	0.2974(1)	2.77(2)
O(1)	0.2359(2)	0.2109(2)	0.3753(2)	4.61(7)
O(2)	0.6458(3)	−0.1544(2)	0.2552(3)	6.14(10)
C(1)	0.2924(2)	0.2929(2)	0.1424(2)	3.09(7)
C(2)	0.1865(3)	0.1694(2)	0.0618(2)	3.99(8)
C(3)	0.0643(3)	0.1561(3)	−0.0578(3)	5.12(10)
C(4)	0.0450(3)	0.2635(3)	−0.0980(3)	5.34(11)
C(5)	0.1484(3)	0.3859(3)	−0.0202(3)	4.78(10)
C(6)	0.2715(3)	0.4003(2)	0.1003(2)	3.88(8)
C(7)	0.6299(2)	0.3289(2)	0.2483(2)	2.99(7)
C(8)	0.6247(3)	0.2440(3)	0.1228(2)	4.19(9)
C(9)	0.7540(3)	0.2560(3)	0.0880(3)	4.88(11)
C(10)	0.8879(3)	0.3548(3)	0.1785(3)	4.49(10)
C(11)	0.8916(3)	0.4419(3)	0.3019(3)	4.28(9)
C(12)	0.7639(3)	0.4288(2)	0.3377(2)	3.45(8)
C(13)	0.4510(2)	0.1489(2)	0.3088(2)	3.15(7)
C(14)	0.3315(3)	0.1128(2)	0.3469(2)	3.45(7)
C(15)	0.3170(3)	−0.0149(2)	0.3526(2)	3.88(8)
C(16)	0.4178(3)	−0.1078(2)	0.3203(2)	4.15(9)
C(17)	0.5358(3)	−0.0723(2)	0.2852(3)	4.02(8)
C(18)	0.5529(3)	0.0567(2)	0.2797(2)	3.64(8)
C(19)	0.1088(3)	0.1774(3)	0.4081(3)	5.38(11)
C(20)	0.6131(5)	−0.2955(3)	0.2302(4)	6.91(16)

[a] B_{eq} (Å^2) is the isotropic equivalent of the anisotropic temperature factor.

phorus atom geometries in **1** and **2** are similar suggesting that minimal disruption is caused by rotation of the hydroquinonyl substituents.

2.1.2. Crystal structures

trans-[PdCl₂(pphqH₂)₂]·(acetone)₂. The crystal structure of $(1)\cdot(\text{acetone})_2$ consists of infinite two-dimensional layers of **1** formed by intermolecular hydrogen

Table 8
Bond lengths (Å) for **3** with e.s.d.s in parentheses

Pd–Cl	2.307(1)	C(9)–C(10)	1.389(4)
Pd–P	2.337(1)	C(10)–C(11)	1.375(4)
Pd–Cl [a]	2.307(1)	C(11)–C(12)	1.386(3)
Pd–P [a]	2.337(1)	C(12)–C(7)	1.393(3)
P–C(1)	1.825(2)	C(13)–C(14)	1.408(3)
P–C(7)	1.826(2)	C(14)–C(15)	1.381(3)
P–C(13)	1.821(2)	C(15)–C(16)	1.384(3)
C(1)–C(2)	1.394(3)	C(16)–C(17)	1.369(3)
C(2)–C(3)	1.383(4)	C(17)–C(18)	1.397(3)
C(3)–C(4)	1.364(4)	C(18)–C(13)	1.379(3)
C(4)–C(5)	1.373(4)	C(14)–O(1)	1.374(3)
C(5)–C(6)	1.390(4)	O(1)–C(19)	1.418(3)
C(6)–C(1)	1.378(3)	C(17)–O(2)	1.377(3)
C(7)–C(8)	1.384(3)	O(2)–C(20)	1.417(3)
C(8)–C(9)	1.390(3)		

[a] Refers to the symmetry transformation $1-x$, $1-y$, $1-z$.

Table 9
Bond angles (°) for **3** with e.s.d.s in parentheses

Cl–Pd–P	94.1(1)	C(7)–C(8)–C(9)	120.2(2)
Cl [a]–Pd–P	85.9(1)	C(8)–C(9)–C(10)	120.0(2)
Pd–P–C(1)	120.9(1)	C(9)–C(10)–C(11)	120.0(2)
Pd–P–C(7)	110.5(1)	C(10)–C(11)–C(12)	120.1(2)
Pd–P–C(13)	112.7(1)	C(11)–C(12)–C(7)	120.3(2)
C(1)–P–C(7)	101.0(1)	P–C(13)–C(14)	118.2(2)
C(1)–P–C(13)	103.9(1)	P–C(13)–C(18)	122.5(2)
C(7)–P–C(13)	106.3(1)	C(18)–C(13)–C(14)	119.3(2)
P–C(1)–C(2)	122.9(2)	C(13)–C(14)–C(15)	119.5(2)
P–C(1)–C(6)	118.6(2)	C(13)–C(14)–O(1)	115.6(2)
C(6)–C(1)–C(2)	118.5(2)	C(15)–C(14)–O(1)	124.9(2)
C(1)–C(2)–C(3)	120.2(2)	C(14)–C(15)–C(16)	120.6(2)
C(2)–C(3)–C(4)	120.7(2)	C(15)–C(16)–C(17)	120.0(2)
C(3)–C(4)–C(5)	120.0(2)	C(16)–C(17)–C(18)	120.1(2)
C(4)–C(5)–C(6)	119.8(3)	C(16)–C(17)–O(2)	125.1(2)
C(5)–C(6)–C(1)	120.9(2)	C(18)–C(17)–O(2)	114.8(2)
P–C(7)–C(8)	121.4(2)	C(17)–C(18)–C(13)	120.4(2)
P–C(7)–C(12)	119.3(2)	C(14)–O(1)–C(19)	118.0(2)
C(12)–C(7)–C(8)	119.3(2)	C(17)–O(2)–C(20)	116.8(2)

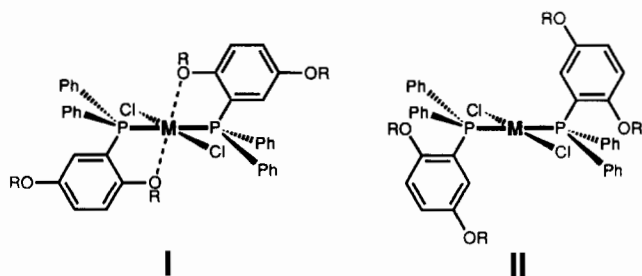[a] Refers to the symmetry transformation $1-x$, $1-y$, $1-z$.

Fig. 4. Diagram showing alternative conformations for the hydroquinonyl substituents in 1–3.

bonding between the hydroquinonyl oxygen atom OC12 and the hydroquinonyl oxygen atom OC15 of an adjacent molecule of **1**, Fig. 5. Each layer has $P2_1/a$ symmetry, but disorder in the stacking of the individual layers leads to the observed $C2/m$ crystallographic symmetry (see Section 4 for details). The hydrogen atom attached
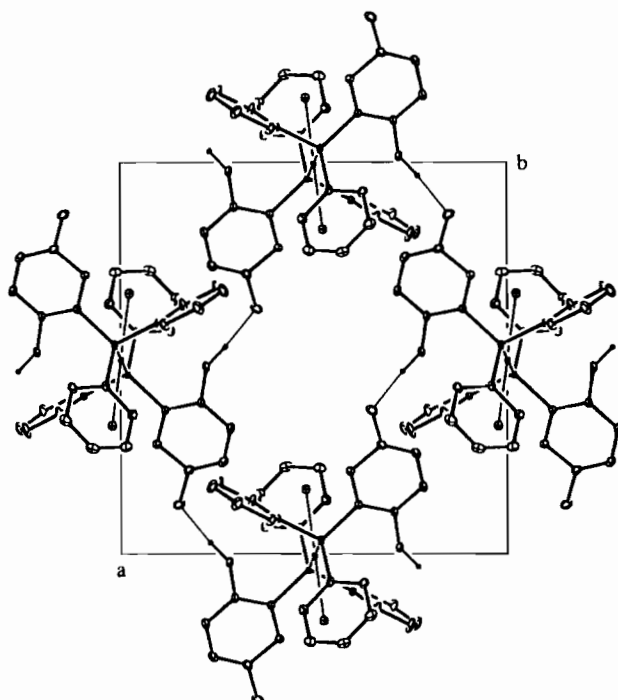

Fig. 5. View of the crystal structure of (**1**)·(acetone)$_2$ showing the two-dimensional layers of **1** formed by intermolecular hydrogen bonding between adjacent molecules of **1**.

to OC12 was located but the hydrogen atom attached to OC15 was not specifically located. This hydrogen atom appears to hydrogen bond to one of the disordered lattice acetone molecules which lie within the cavity formed by the four molecules of **1** (Fig. 5). In the crystal structure, the layers of **1** lie on top of each other thus producing acetone filled channels that run parallel to the c axis. The lattice acetone molecules were disordered and were not located but rather the solvent region was modelled using back Fourier transform techniques [13].

trans-[PtCl$_2$(pphqH$_2$)$_2$] · (*dimethylformamide*)$_4$. (**2**) · (DMF)$_4$ crystallizes in the triclinic space group $P\bar{1}$. The pattern of the hydrogen bonding in the crystal structure of (**2**)·(DMF)$_4$ is different from that in the crystal structure of (**1**)·(acetone)$_2$. In (**2**)·(DMF)$_4$, each hydroquinonyl group is hydrogen bonded through oxygen atoms, O(1) and O(2) to two dimethylformamide oxygen atoms, D10 and D20, respectively. The resulting unit cell which contains **2** and its four hydrogen bonded dimethylformamide molecules is shown in Fig. 6. There is no hydrogen bonding between the (**2**)·(DMF)$_4$ units in the crystal structure.

trans-[PdCl$_2$(pphqMe$_2$)$_2$]. Complex **3** crystallizes without included solvent in the triclinic space group $P\bar{1}$. There is one molecule of **3** in the unit cell and there are no close intermolecular contacts throughout the crystal structure.
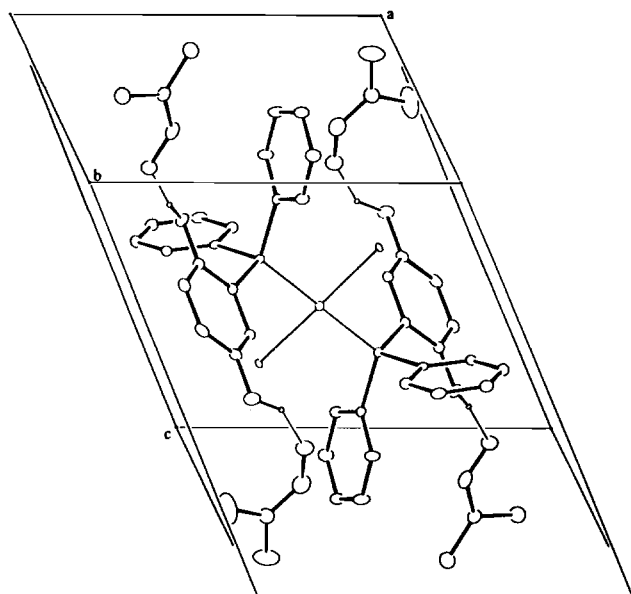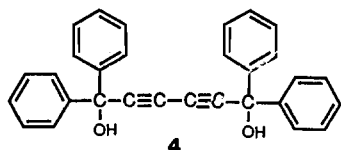
Fig. 6. View of the unit cell of (2)·(DMF)₄.

Fig. 7. Schematic diagram of organic (entry 1) and inorganic (entries 2–4) 'wheel (A)-and-axle (B)' host molecules.

3. Discussion

Compounds likely to behave as lattice inclusion hosts, or functional group-assisted hosts, are generally unable to pack efficiently by themselves, leaving volumes of space which are occupied by the guest molecules [14]. In the deliberate design of such compounds a number of synthetic strategies have been employed to achieve these ends. One approach is to employ a hydrogen bonding motif which is likely to result in a low-density host network [15]. Alternatively, the shape of the host may be selected. Thus the 'scissor-like' and 'roof-shaped' hosts developed by Weber [16] have proved to be a fruitful source of new inclusion materials.

Likewise the 'wheel-and-axle' compounds of Toda and Hart and co-workers have also become recognized as being a major structural class of hosts [7–9]. This family of materials is constructed from two bulky and relatively rigid end groups (wheels) separated by a rigid connecting link (axle) as shown diagrammatically in Fig. 7. Common end groups include diaryl, triaryl or tryptycyl moieties; whereas connecting links include allenyl, alkenyl, alkynyl or azo groups. The presence of hydrogen bonding groups is not always obligatory for the compounds to exhibit inclusion behavior [8,14]. Arguably the best known example of this series is the diacetylenic diol 4, but a wide variety of compounds has been investigated [17].

4

The hydroquinonylphosphine complexes 1–3 reported here have 'wheel-and-axle' topology, albeit with a
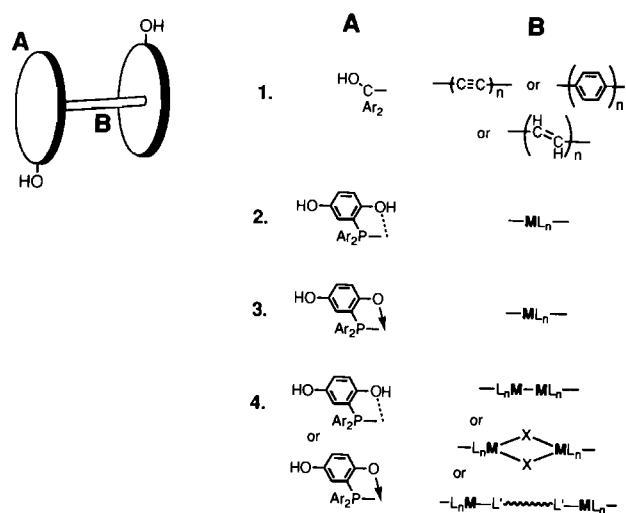
short axle consisting only of a dichloropalladium or dichloroplatinum unit separating the two bulky triarylphosphine groups. A more graphic description would be to name these as 'dumb-bell' shaped molecules.

As already described, molecules of 1 in (1)·(acetone)₂ hydrogen bond to produce layers which are stacked in a disordered manner. However, the cavities enclosed by four adjacent hydrogen-bonded molecules are also stacked to produce parallel channels containing the acetone-guest. The hydrogen atom on OC15 probably forms a hydrogen bond to the acetone, thus stabilizing the host–guest combination and leading to the observed stoichiometry. This inclusion compound therefore exists due to a combination of lattice and coordination factors. It is best described as a functional group-assisted coordinato-clathrate [18] with tubulate topology [19].

In general topological terms this structure has many similarities with that of the compound formed by the diacetylenic diol 4 with acetone [8]. This substance, with the same stoichiometry (host)·(acetone)₂, also results in open channels roughly parallel to the long axis of the host molecule. These canals also contain acetone which is complexed via $-O-H...O=C\langle$ hydrogen bonds [8,14].

Crystallization of 2 from dimethylformamide gave (2)·(DMF)₄ with each hydroquinonyl hydroxy group involved in $-O-H...O=C\langle$ hydrogen bonding to a dimethylformamide molecule. In doing so the attractive interaction between the *ortho* $-O-H$ group and the metal atom observed in (1)·(acetone)₂ (vide supra) has been lost. Clearly the interaction of the hydroxy groups with the metal is less favorable than hydrogen bonding to dimethylformamide. This substance is best described as an inclusion complex between 2 and dimethylformamide, leading to discrete (2)·(DMF)₄ units which close-pack without hydrogen bonding to form the crystal lattice.

In contrast to the earlier results, the dimethoxyphenylphosphine complex 3 crystallizes as guest-free material. The methoxy group *ortho* to the phosphorus atom is oriented towards the metal atom as for 1, but the absence of hydroxy groups precludes formation of a hydrogen bonded network or hydrogen bonds to guest molecules. This finding suggests that the 'dumb-bell' topology alone is perhaps insufficient to induce inclusion behavior in the series of molecules.

Nevertheless, the behavior of complexes 1–3 affords valuable information towards the design and prediction of new inorganic host complexes. Fig. 7 shows a schematic diagramatic representation of the 'wheel-and-axle' host concept, together with examples of typical wheel (A) and axle (B) sub-structures. Entry 1 summarizes well-established organic examples of this principle [8,10]; entry 2 includes compounds 1 and 2; while entries 3 and 4 represent postulated inorganic extensions of the concept.

Minor variations to the ligand (L), aromatic group (Ar), or coordinated donor atom (e.g. changing from P to As, or more dramatically, going from phosphine to bulky thiol), clearly should result in further examples of inclusion behavior. More fundamentally, permanent bonding (rather than a reversible attractive interaction in solution) between the hydroquinonyl unit and the metal would increase the rigidity of the host unit. Toda's results with purely organic systems indicate that this property is significant [20], and our results show that permanent coordination of the hydroquinonyl *ortho*-oxygen atom to the metal can be achieved by pH or electrochemical control [1,2]. Alteration of the axle length by use of two (or more) metal centers could be achieved in a linear fashion in metal–metal bonded species $(-L_nM-ML_n-)$, but the use of ligand bridged metal dimers with bridging ligands $(-L_nM(\mu-X)_2ML_n-)$ would assure concomitant rigidity of the 'wheel-and-axle' topology. We have recently prepared coordinated hydroquinonyl complexes, $[(O,P-pphqH)Pd(\mu-X)_2Pd(O,P-pphqH_2)]$ (X = Cl, Br, I), which fit this structural motif [21]. The axle length would be most readily controlled in dimers, $-L_nM(\mu-L' \sim L')ML_n-$ spanned by bridging ligands $(\mu-L' \sim L')$ such as, for example, pyrazine, 4,4'-bipyridine or 4,4'-bis(diphenylphosphino)biphenylene. We therefore predict that structures based on entries 3 and 4 are likely candidates for the deliberate design of new inorganic inclusion materials.

4. Experimental

The preparative procedures and the microanalytical and spectroscopic data for 1–3 are reported elsewhere [1,2]. Yellow–orange rhombs of (1)·(acetone)$_2$ were obtained by slow evaporation of an acetone solution of 1. Pale yellow blocks of (2)·(DMF)$_4$ were obtained by very slowly cooling a warm solution of 2 in dimethylformamide under an atmosphere of dichloromethane vapour. Yellow rhombs of 3 were crystallized from a concentrated dichloromethane solution of the complex.

4.1. X-ray crystallography

A summary of the crystal data is presented in Table 10.

4.1.1. Structure determination for (2)·(DMF)$_4$ and 3

Reflexion data were measured with an Enral-Nonius CAD-4 diffractometer in $\theta/2\theta$ scan mode using graphite monochromatized molybdenum radiation (λ 0.7107 Å). Data were corrected for absorption. Reflections with $I > 3\sigma(I)$ were considered observed. The structures were determined by direct phasing and Fourier methods. Phenyl hydrogen atoms were included in calculated positions, the remainder located in difference Fouriers, and were assigned thermal parameters equal to those of the atom to which it bonded. Positional and anisotropic thermal parameters for the non-hydrogen atoms were refined using full-matrix least-squares. Reflexion weights used were $1/\sigma^2(F_o)$, with $\sigma(F_o)$ being derived from $\sigma(I_o) = [\sigma^2(I_o) + (0.04I_o)^2]^{1/2}$. The weighted residual is defined as $R_w = (\Sigma w\Delta^2/\Sigma wF_o^2)^{1/2}$. Atomic scattering factors and anomalous dispersion parameters were from International Tables for X-ray Crystallography [22]. Structure solution was by MULTAN80 [23] and refinement used BLOCKLS, a local version of ORFLS [24]. ORTEP-II [25] running on a Macintosh IIcx was used for the structural diagrams, and an IBM 3090 computer was used for calculations.

4.1.2. Structure solution for (1)·(acetone)$_2$

Reflexion data were measured with an Enraf-Nonius CAD-4 diffractometer in $\theta/2\theta$ scan mode using graphite monochromatized molybdenum radiation (λ 0.7107 Å). Data were corrected for absorption. Reflexions with $I > 3\sigma(I)$ were considered observed.

The disordered structure can be regarded as corresponding to either $l = 2n$ only data of an ordered structure in space group $I2/a$, $\mathbf{a}' = \mathbf{a}$, $\mathbf{b}' = \mathbf{b}$, $\mathbf{c}' = 2\mathbf{c}$, $Z = 4$ [$I2/a$ hkl: $h+k+l = 2n$ only, $h0l$: $h = 2n$ ($l = 2n$) only becomes $C2/m$ hkl: $h+k = 2n$ only, $h0l$: ($h = 2n$) only if $l = 2n$ only is observed] or $h+k = 2n$ only data of an ordered structure in space group $P2_1/a$, $\mathbf{a}'' = \mathbf{a}$, $\mathbf{b}'' = \mathbf{b}$, $\mathbf{c}'' = \mathbf{c}$, $Z = 2$ [$P2_1/a$ $h0l$: $h = 2n$ only, $0k0$, $k = 2n$ only becomes $C2/m$ $h0l$: ($h = 2n$) only, $0k0$ ($k = 2n$) only if $h+k = 2n$ only is observed].

The justification for this assumption is based on the idea that a sensible layer of ordered molecules perpendicular to $\mathbf{c}^*$ can be constructed. This layer is connected by an infinite two-dimensional network of

Table 10
Crystal data for (**1**)·(acetone)$_2$, (**2**)·(DMF)$_4$ and **3**

	(**1**)·(acetone)$_2$	(**2**)·(DMF)$_4$	**3**
Empirical formula	$C_{42}H_{42}Cl_2O_6P_2Pd$	$C_{48}H_{58}Cl_2N_4O_8P_2Pt$	$C_{40}H_{38}Cl_2O_4P_2Pd$
M	882	1147	822
Crystal size (mm)	$0.10 \times 0.13 \times 0.15$	$0.08 \times 0.10 \times 0.13$	$0.14 \times 0.17 \times 0.22$
Crystal class	monoclinic	triclinic	triclinic
Space group	$C2/m$	$P\bar{1}$	$P\bar{1}$
Z	2	1	1
a (Å)	13.857(6)	10.500(6)	9.063(5)
b (Å)	13.589(3)	11.927(8)	10.548(7)
c (Å)	11.863(5)	12.225(6)	11.596(8)
α (°)		64.65(5)	111.57(3)
β (°)	104.68(2)	66.74(5)	111.26(3)
γ (°)		78.84(5)	90.09(4)
V (Å^3)	3949(2)	1271(1)	949(1)
D_{calc} (g cm^{-1})	1.36	1.50	1.44
Min., max., transmission factors	0.91, 0.94	0.67, 0.76	0.85, 0.89
μ_{Mo} (cm^{-1})	6.62	30.08	7.44
$2\theta_{max}$ (°)	45	50	50
No. unique data	1482	4459	3329
No. observed reflections	1268	4302	3031
Final R	0.058	0.046	0.021
Final R_w	0.072	0.065	0.035

hydrogen bonds and has $P2_1/a$ symmetry (see Fig. 5) with the Pd atoms at centers of inversion separated by $(\mathbf{a}+\mathbf{b})/2$. These sites become $2/m$ sites in the disordered $C2/m$ structure. The next hydrogen bonded layer can be related by a translation of either $\mathbf{c}$ to create space group $P2_1/a$ or $(\mathbf{a}+\mathbf{b}+\mathbf{c}')/2$ where $\mathbf{c}'=2\mathbf{c}$ to create space group $I2/a$. Stacking faults cause only the reflections associated with the $C2/m$ disordered structure to be observed. The relative positions of the Pd atoms are not dependent on the stacking of layers and the complex packs in columns parallel to $\mathbf{c}$ with the P–Pd–P direction almost parallel to $\mathbf{c}$. The hydrogen bonding network causes a large space to be left between the columns. The crystal was grown from an acetone solution and two acetones per formula unit co-crystallize in the region about the line $\frac{1}{2}, \frac{1}{2}, z$ in the unit cell. The stacking fault will naturally cause a disordering of the solvent but it appears that a simple 1:1 disordering does not occur but rather a more haphazard filling of the available space.

If no scattering material is included in the region of the solvent then refinement produced values for R and R_w of 0.085 and 0.125 for the observed, $I > 3\sigma(I)$, data. When segmented by $\sin \theta/\lambda$ range values of 0.370 and 0.486 were obtained for the 10 data with $\sin \theta/\lambda < 0.1$, 0.1572 and 0.2324 for the 66 data with $0.1 < \sin \theta/\lambda < 0.2$ and 0.074 and 0.098 for the remaining 1191 observed data. Values of 0.999 and 0.469 were obtained for the 215 data with $I < 3\sigma(I)$. The solvent region was considered unparamaterizable and was therefore modelled by back Fourier transform [26] and included in the structure factor calculation for least-squares re-

finement using the constrained least-squares refinement program RAELS [27]. This procedure produced values for R and R_w of 0.58 and 0.072 for the $I > 3\sigma(I)$ data and upon segmentation produced values of 0.088 and 0.101; 0.092 and 0.117; 0.054 and 0.065 for the $\sin \sigma/\lambda$ ranges as before and 0.468 and 0.260 for the $I < 3\sigma(I)$ data. The contribution of the back Fourier transform to the $F(000)$ reflection was consistent with two acetones per formula unit. Space filling arguments and density measurement supported this hypothesis. We note that only low angle data is sensitive to the solvent in the structure, the effect on data with $\sin \theta/\lambda < 0.1$ being quite dramatic. The Pd, Cl and P atoms were refined as isolated anisotropic atoms with the U_{12} and U_{13} parameters constrained to be zero. Constraints were used in the refinement of the remaining atoms in the complex. Atoms of the three ring systems attached to the P atom were constrained to be planar with the two phenyl groups constrained to be equal and have $mm2$ local symmetry. Local coordinates for atoms in the group were refined within these limitations. A refined 12 parameter TL libration model centered on the P atom was used to describe the anisotropic thermal parameters of atoms in a particular ring system, one such model being used per ring system. The phenyl ring H atoms were constrained to lie at geometrically sensible positions and included in the liberating ring systems for anisotropic thermal parameter evaluation. The H atom attached to the O(1) atom was located in its hydrogen bond to atom O(2) in an adjacent molecule but the H attached to O(2) was not specifically located. This H atom would appear to hydrogen bond

to an O atom of an acetone in the solvent region and is not well defined as the solvent region is not well defined.

5. Supplementary material

Tables of fractional coordinates, isotropic thermal parameters for hydrogen atoms, anisotropic thermal parameters for non hydrogen atoms, bond distances and angles, torsional angles, and observed and calculated structure factors for all three crystal structures are available on request from author D.C.C.

References

[1] S.B. Colbran, D.C. Craig and S.B. Sembiring, *Inorg. Chim. Acta*, *176* (1990) 225; S.B. Sembiring, S.B. Colbran and L.R. Hanton, *Inorg. Chim. Acta*, *202* (1992) 67.

[2] S.B. Sembiring, S.B. Colbran and D.C. Craig, submitted for publication.

[3] D.D. MacNicol, in J.L. Atwood, J.E.D. Davies and D.D. MacNicol (eds.), *Inclusion Compounds*, Vol. 2, Academic Press, London, 1984, Ch. 1, pp. 1–45.

[4] D.E. Palin and H.M. Powell, *J. Chem. Soc.*, (1974) 208, (1948) 815; H.M. Powell, *J. Chem. Soc.*, (1948) 61; (1950) 298, 300.

[5] O. Ermer, *Helv. Chim. Acta*, *74* (1991) 1939.

[6] J.L. Atwood, J.E.D. Davies and D.D. MacNicol (eds.), *Inclusion Compounds*, Vol. 1, Academic Press, London, 1984, Vol. 5, Oxford University Press, Oxford, 1991.

[7] F. Toda and K. Agaki, *Tetrahedron Lett.*, (1968) 3695.

[8] F. Toda, D.L. Ward and H. Hart, *Tetrahedron Lett.*, *22* (1981) 3865.

[9] H. Hart, L.-T.W. Lin and D.L. Ward, *J. Am. Chem. Soc.*, *106* (1984) 4043.

[10] E. Weber, K. Skobridis, A. Wierig, L.R. Nassimbeni and L. Johnson, *J. Chem. Soc., Perkin Trans.*, 2 (1992) 2123.

[11] F. Maassarani, M. Pfeffer and G. Le Borgne, *Organometallics*, *6* (1987) 2043; F. Balegroune, P. Braunstein, T.M.G. Carneiro, D. Grandjean and D. Matt, *J. Chem. Soc.*, (1989) 582; N.W. Alcock, A.W.G. Platt and P.G. Pringle, *J. Chem. Soc., Dalton Trans.*, (1987) 2273 and (1989) 139.

[12] G.A. Bowmaker, J.D. Cotton, P.C. Healy, J.D. Kildea, S.B. Silong, B.W. Skelton and A.H. White, *Inorg. Chem.*, *28* (1989) 1462, and refs. therein.

[13] A.T. Baker and A.D. Rae, *Acta Crystallogr., Sect. A*, *40* (Suppl.) (1984) 17.4-4.

[14] I. Goldberg, *Top. Curr. Chem.*, *149* (1988) 1.

[15] R. Bishop. D.C. Craig, I.G. Dance, M.L. Scudder, A.P. Marchand and Y. Wang, *J. Chem. Soc., Perkin Trans.* 2, (1993) 937; R. Bishop, D.C. Craig, I.G. Dance, S. Kim, M.A.I. Mallick, K.C. Pich and M.L. Scudder, *Supramol. Chem.*, *1* (1993) 171.

[16] E. Weber and M. Czugler, *Top. Curr. Chem.*, *149* (1988) 45; E. Weber, in J.L. Atwood, J.E.D. Davies and D.D. MacNicol (eds.), *Inclusion Compounds*, Vol. 4, Oxford University Press, Oxford, 1991, Ch. 5, pp. 188–262.

[17] F. Toda and K. Agaki, *Tetrahedron Lett.*, (1968) 2695.

[18] E. Weber, I. Csöregh, B. Stensland and M. Czugler, *J. Am. Chem. Soc.*, *106* (1984) 3297.

[19] E. Weber and H.-P. Josel, *J. Incl. Phenom.*, *1* (1983) 79.

[20] F. Toda, in J.L. Atwood, J.E.D. Davies and D.D. MacNicol (eds.), *Inclusion Compounds*, Vol. 4, Oxford University Press, Oxford, 1991, Ch. 4, pp. 126–187.

[21] S.B. Sembiring, *Ph.D. Thesis*, University of New South Wales, Australia, 1993.

[22] J.A. Ibers and W.C. Hamilton (eds.), *International Tables for X-Ray Crystallography*, Vol. 4, Kynoch, Birmingham, UK, 1974.

[23] P. Main, *MULTAN80*, University of York, UK, 1980.

[24] W.R. Busing, K.O. Martin and H.A. Levy, *ORFLS*, Oak Ridge National Laboratory, TN, 1962.

[25] C.K. Johnson, *ORTEP-II*, Oak Ridge National Laboratory, TN, 1976.

[26] A.D. Rae and A.T. Baker, *Acta Crystallogr., Sect. A*, 40 (Suppl.) (1984) C428.

[27] A.D. Rae, *RAELS89*, a comprehensive constrained least squares refinement program, University of New South Wales, Australia, 1989.